

Article

Diavik Waste Rock Project: Evolution of Mineral Weathering, Element Release, and Acid Generation and Neutralization during a Five-Year Humidity Cell Experiment

Jeff B. Langman ^{1,*}, Mandy L. Moore ^{1,2}, Carol J. Ptacek ¹, Leslie Smith ³, David Segó ⁴ and David W. Blowes ¹

¹ Department of Earth and Environmental Sciences, University of Waterloo, Waterloo, ON N2L 3G1, Canada; E-Mails: mandy.moore@uwaterloo.ca (M.L.M.); ptacek@uwaterloo.ca (C.J.P.); blowes@uwaterloo.ca (D.W.B.)

² Comco Canada Inc., Barrie, ON L4N 8Y4, Canada

³ Department of Earth, Ocean, and Atmospheric Sciences, University of British Columbia, Vancouver, BC V6T 1Z4, Canada; E-Mail: lsmith@eos.ubc.ca

⁴ Department of Civil and Environmental Engineering, University of Alberta, Edmonton, AB T6G 2W2, Canada; E-Mail: dave.sego@ualberta.ca

* Author to whom correspondence should be addressed; E-Mail: jlangman@uwaterloo.ca; Tel.: +1-519-888-4567.

Received: 30 January 2014; in revised form: 29 March 2014 / Accepted: 1 April 2014 /

Published: 10 April 2014

Abstract: A five-year, humidity-cell experiment was used to study the weathering evolution of a low-sulfide, granitic waste rock at 5 and 22 °C. Only the rock with the highest sulfide content (0.16 wt %) released sufficient acid to overcome a limited carbonate acid-neutralization capacity and produce a substantial decline in pH. Leached SO₄ and Ca quickly increased then decreased during the first two years of weathering. Sulfide oxidation continued to release acid and SO₄ after carbonate depletion, resulting in an increase in acid-soluble elements, including Cu and Zn. With the dissolution of Al-bearing minerals, the pH stabilized above 4, and sulfide oxidation continued to decline until the end of the experiment. The variation in activation energy of sulfide oxidation correlates with changes in sulfide availability, where the lowest activation energies occurred during the largest releases of SO₄. A decrease in sulfide availability was attributed to consumption of sulfide and weathered rims on sulfide grains that reduced the oxidation rate. Varying element release rates due to changing carbonate and sulfide availability provide identifiable

geochemical conditions that can be viewed as neutralization sequences and may be extrapolated to the field site for examining the evolution of mineral weathering of the waste rock.

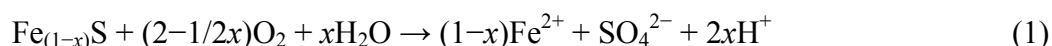
Keywords: humidity cell; rock acid generation; mineral acid neutralization; element release rates; pyrrhotite activation energy

1. Introduction

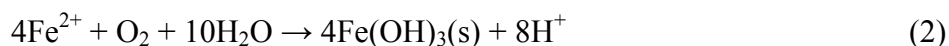
The oxidation of sulfide minerals in waste rock can produce acid rock drainage (ARD), which is characterized by low pH, elevated SO_4 concentrations, and the mobilization of elements such as Co, Cu, Fe, Ni, and Zn that are typically less mobile under neutral pH conditions [1–3]. The Diavik Waste Rock Project is a multidisciplinary research program implemented to examine the potential for ARD in an Arctic region through the study of the weathering of various laboratory and field samples of a low-sulfide, run-of-mine waste rock. A significant part of the project was a long-term (years), humidity-cell experiment to examine the generation of ARD, acid neutralization, and element release rates from the accelerated weathering of small-scale samples of waste rock under different temperatures. Insight into the mobilization/immobilization of oxidation products assists in understanding the generation of ARD, which may occur over periods of years to decades to centuries [2,4–6]. The utility of this long-term, humidity-cell experiment is the identification of possible changes in leachate chemistry due to changes in the availability of acid-generating and acid-neutralizing minerals that provide a temporal trend of neutralization sequences for evaluation of field conditions.

A weathering or release rate is the rate at which primary minerals are transformed to secondary minerals or dissolved reaction products, congruently or incongruently, with release of elements [7]. Predicting field conditions from humidity-cell results can be difficult because of coupled and sustained biogeochemical processes in the field that create a more complex environment than can be reproduced in the laboratory [2,8–11]. Although, the fine fraction material (<6.3 mm) used for humidity cells is representative of the grain-size fraction likely to undergo the greatest weathering in the field because of the large available reactive surface area in these grains [12,13]. The purpose of the humidity-cell experiment was to examine release rates and evaluate the temporal change of the geochemical environment on the humidity-cell scale and how this might be related to field conditions.

With the exposure of sulfide minerals such as pyrrhotite [$\text{Fe}_{(1-x)}\text{S}$] to moisture and oxygen, oxidation will produce Fe^{2+} , SO_4 , and H^+ (Equation (1)).



Oxidation of Fe^{2+} to Fe^{3+} , followed by hydrolysis and precipitation of ferric (oxyhydr)oxides represented here as $\text{Fe}(\text{OH})_3$, may occur with additional oxygen and water (Equation (2)).



Numerous intermediary or end products, such as goethite [$\alpha\text{-FeO}(\text{OH})$], lepidocrocite [$\gamma\text{-FeO}(\text{OH})$], akaganéite [$\beta\text{-FeO}(\text{OH})$], ferrihydrite [$(\text{Fe}_2\text{O}_3 \cdot 0.5\text{H}_2\text{O})$], magnetite [$\text{Fe}^{2+}\text{Fe}^{3+}_2\text{O}_4$], and hematite [Fe_2O_3],

are possible with oxidation of Fe^{2+} . The oxidation of Fe^{2+} produces additional acidity, although this reaction is influenced by Fe^{3+} mineral speciation and pH and generally requires an oxic environment [14].

Dissolution of minerals such as calcite [CaCO_3], Al and Fe hydroxides, and aluminosilicates are common acid-neutralizing reactions observed in mine wastes [3,15]. These minerals are consumed at different rates according to their reactivity—aluminosilicate (e.g., feldspars) dissolution begins at near neutral pH, but the weathering rate is substantially slower compared to carbonate weathering [16]. Carbonate dissolution rates [17] generally are higher than oxidation-dissolution rates of sulfides such as pyrrhotite [18], but the neutralization capacity of the carbonate system will be limited by the mineral concentration and availability in the rock compared to sulfide minerals [3]. The variation in availability of acid-producing and acid-neutralizing minerals and their different reactivities produces acid-neutralization sequences where different minerals become the dominant acid neutralizer as mineral availability changes [3,6,12,15].

2. Site Description

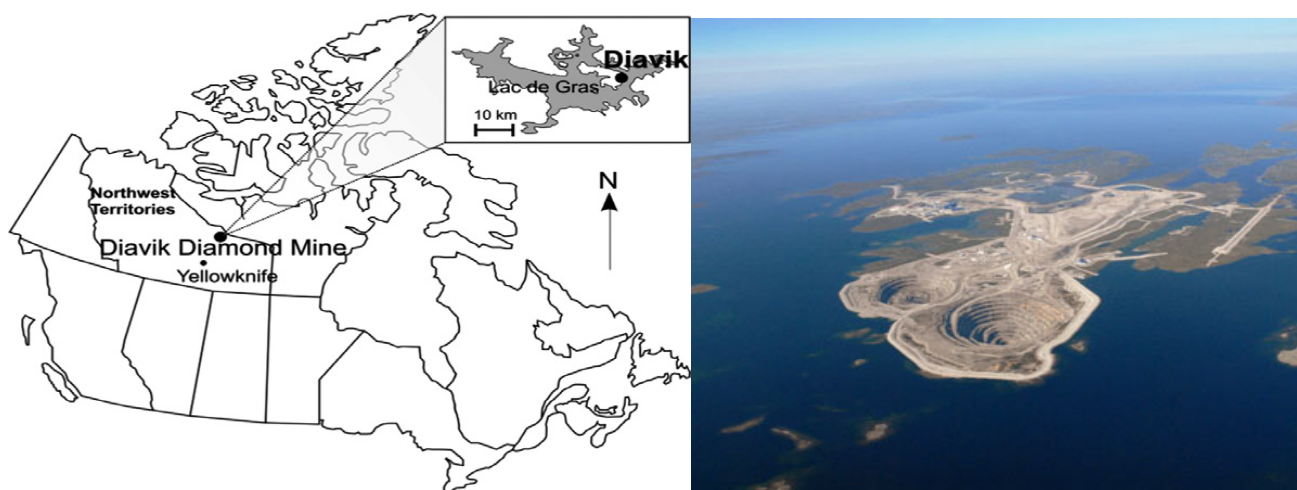
The Diavik Diamond Mine (Diavik) is located on an island in Lac de Gras in the Northwest Territories, Canada (Figure 1). The Diavik site is located in the Canadian Arctic—a permafrost, polar-climate region with an annual precipitation of less than 300 mm (40% as rain, 60% as snow), and mean annual minimum, average, and maximum temperatures of -31 , -9 , 18 °C, respectively [19]. Open-pit and underground mining has been used to access diamond-bearing kimberlite ore. The waste (gangue) rock is composed of about 75% granite, 14% pegmatitic granite (pegmatite), 10% biotite schist, and 1% diabase dykes [20]. The granites are primarily quartz [SiO_2], K-feldspar [KAlSi_3O_8], and albite [$\text{NaAlSi}_3\text{O}_8$], with greater albite in the granite and greater K-feldspar in the pegmatite [21]. The biotite schist is composed primarily of albite (35%–55%), quartz (20%–50%), and biotite [$\text{KMg}_3\text{AlSi}_3\text{O}_{10}(\text{OH})_2$] (10%–25%) and has a mean sulfide content of 0.24 as wt % S (range of 0.02–0.42 wt % S). The sulfide is largely pyrrhotite (typically 100–200 μm) with traces of pyrite [FeS_2], chalcopyrite [CuFeS_2], and sphalerite [$(\text{Zn},\text{Fe})\text{S}$]. Diavik waste rock is segregated prior to disposal according to total S content: Type I, <0.04 wt %; Type II, 0.04 to 0.08 wt %; and Type III, >0.08 wt %.

3. Methods

The humidity-cell experiment consisted of two six-cell sets—one at ambient-room temperature (mean of 22 °C, range of 20–24 °C) and one at cold-storage temperature (mean of 5 °C, range of 4–7 °C)—with two replicate samples of the three rock types in each cell set. Samples of all three rock types (I, II, and III) were collected in October 2004 within 2-days of initial excavation. Waste rock samples were collected through a random selection method using power equipment and/or a shovel per standard practice for sampling aggregates [22], and the samples were subsampled for laboratory use per American Society for Testing and Materials (ASTM) standards [23–25]. Replicate samples were sent to three commercial laboratories for repeated static testing (acid-base accounting [26–28]) including whole-rock analysis for metal-oxide concentrations, paste pH, neutralization potential (NP), acid production (AP), S and C content, and net-acid generation (NAG). The physical characteristics of grain-size distribution, mean surface area (Brunauer–Emmett–Teller (BET) method [29]), and slake

durability [30] were analyzed to evaluate potential weathering characteristics. Samples for humidity-cell construction were sieved to <6.3 mm and dried. Each cell was loaded with 1 kg of waste rock. For data analysis, replicate data sets were combined into single data sets for Type I, II, or III rock at ambient-room (warm) and cold-storage (cold) temperatures.

Figure 1. The Diavik Diamond Mine is located on East Island in Lac de Gras, 300 km northeast of Yellowknife, Northwest Territories, Canada, and 220 km south of the Arctic Circle (photo courtesy of Diavik Diamond Mines, Inc., Yellowknife, Northwest Territories (NWT), Canada).



Prior to cell construction, the presence or absence of Fe- and S-oxidizing bacteria was determined for each rock type. Bacterial enumeration [31] was performed through a 10-fold dilution series of specific media cultures (Fe-oxidizing, neutrophilic S-oxidizing, and acidophilic S-oxidizing) with 1 g of rock inoculated into 5 replicates for each media. The rock samples were unaltered subsamples of the rock used for the humidity cells, and the samples had been cold preserved for preservation of the microbiological community. All inoculated media were incubated for four weeks [32] at room temperature (20–24 °C). The probability that colony-forming bacteria were or were not present in the diluted samples was based on visible bacteria and changes in pH and color compared to a blank dilution series [33].

The weathering cycle for the humidity-cell experiment was based on a weekly schedule of flooding (drip introduction of deionized water), dry air, and wet air [34]. During each week, flooding of the cells with deionized water for leachate sample collection was followed by a 3-day dry period (<10% relative humidity (RH)) and a 3-day wet period (>95% RH). During week 0, the initial flooding consisted of three consecutive 500 mL of water with a leachate sample collected after each flooding. For weeks 1–3, the same flooding/dry air/wet air cycle was used, but two 500-mL floodings were introduced. From week 4 onward, the weathering conditions were standardized to a single 500 mL flooding followed by the same dry-air/wet-air cycle. The residence time of the flooding of each cell was generally about one hour, followed by draining of the cells. The same weekly cycle occurred through the duration of the experiment, although analysis of the leachate was adjusted to longer intervals as the experiment progressed—one week to two weeks to one month to multiple months.

The leachate was analyzed for pH, Eh, and specific conductance with Orion 3-Star meters/probes and filtered (0.45 μm) for analysis of alkalinity, cations, and anions. Alkalinity was determined using a Hach digital titrator, 0.16 N H_2SO_4 , and bromocresol green/methyl red indicator. Dissolved cation concentrations were determined using an iCAP 6000 ICP-OES (Thermo Scientific, Waltham, MA, USA) and an X-Series 2 ICP-MS (Thermo Scientific). Anion concentrations were determined using a Dionex DX600 IC (Thermo Scientific). Quality control and accuracy were checked with instrument blanks, replicate samples, and calibration standards over the course of the experiment.

4. Results and Discussion

4.1. Waste Rock Characteristics

Differences in physical characteristics of the rock types, such as mineral surface availability, will influence oxidation reactions and alter element release rates. Biotite has a low mineral hardness and provides ready fracture and cleavage planes compared to predominant minerals within the granite. Therefore, Type III rock, containing more biotite schist, should weather to smaller grain sizes with a greater surface area faster than the more granitic Type I and II rocks. Results of the grain-size analysis indicate that the Type III rock contained a greater fraction of finer grains (smaller D10; Table 1) likely as a result of greater disintegration during mining. The Type III rock also had the largest surface area (Table 1). Additionally, Type III rock produced the lowest slake durability value (Table 1) indicating it is the weakest of the three rock types; however, the standard deviation for the three replicate samples of each rock type (35.3 ± 2.1 for Type I, 34.2 ± 0.5 for Type II, 33.5 ± 0.3 for Type III) indicates a variability that lessens the distinction between the rock types. Such physical characteristics of the rock suggest that mining and disposal of the Type III rock should produce finer grains and greater surface area for weathering compared to the more competent Type I and II rock.

The distribution of oxide concentrations (Table 1) indicates a similar gross composition of the three rock types. The Type III rock contained five times more sulfide than the Type I and II rocks. The relatively low sulfide content of the Type II rock estimated using the static test is in contrast to its operational categorization (0.04 to 0.08 wt % S). All of the rock types contained small concentrations of carbonate minerals (≤ 0.06 wt %). The aluminosilicate minerals comprising the large majority of the rock (quartz, K-feldspar, and albite) have low acid neutralization potentials. On a comparative scale with calcite representing 100% neutralization, quartz (0%), K-feldspar (0.1%), and albite (0.1%–0.5%) have negligible neutralization capacities [35–37]. The AP of the sulfide and NP of the carbonate provide a means of evaluating the potential for ARD (NP:AP ratio or neutralization potential ratio (NPR)). Rock with an NPR of less than 1 is considered potentially acid generating, and an NPR of 2 or greater is considered not potentially acid generating [38]. Ratios between 1 and 2 are considered uncertain for acid generation. The Type I and Type II rocks have NPRs that indicate the unlikely generation of ARD, and the Type III rock ratio is within the range of uncertainty (Table 1).

4.2. Leachate Characteristics

The highest concentrations of total dissolved solids (measured by specific conductance) for all rock types occurred during the first weeks of the experiment because of very-fine particles (potential to pass

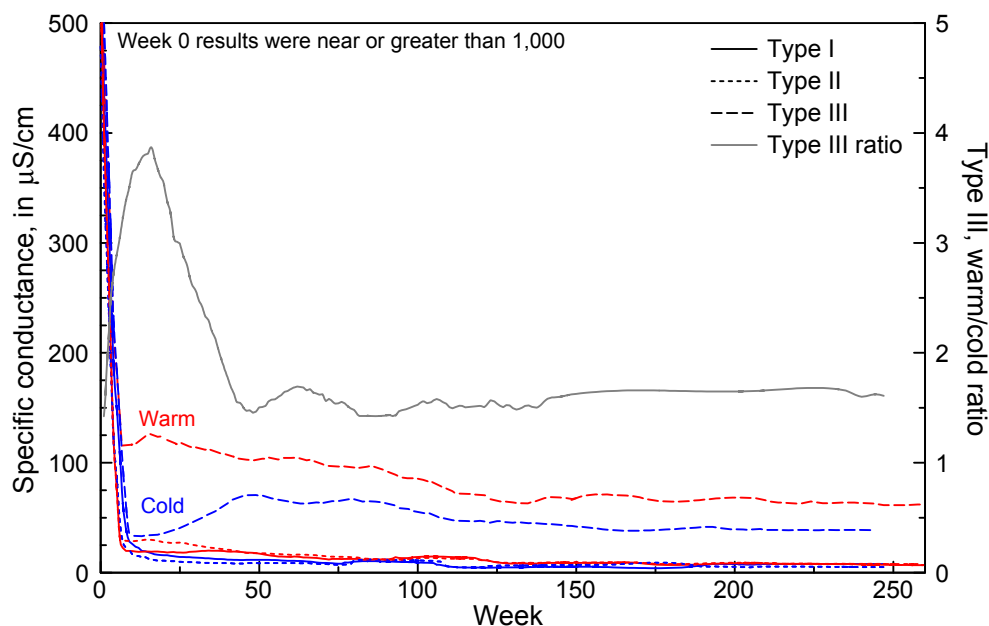
through the cell filter media) and highly reactive fresh-mineral surfaces as a result of mining [39–41]. This effect was anticipated and an increased number of column floodings was implemented for weeks 0, 1, 2 and 3 according to Lapakko and White's [42] modification of the ASTM method [34]. Following the initial release of very-fine particles and early weathering products, the highest concentrations of dissolved solids were observed in the leachate from the Type III rock, particularly in the warm cells (Figure 2). The weathering rate of the Type III rock remained elevated compared to the Type I and II rock for the duration of the experiment.

Table 1. Grain characteristics, metal oxide concentrations, and acid-base accounting results for run-of-mine samples collected in 2004 from Diavik Diamond Mine, Northwest Territories, Canada: D50, median particle size; D10, particle size at which 10% of the grains are smaller; Slake durability, average slake durability index for <6.3-mm particles; NP, neutralization potential; AP, acid generation potential; NAG, net acid generation.

Constituent	Units	Type I ¹	Type II ¹	Type III ¹
D50	µm	2400	2800	2750
D10	µm	150	150	130
Mean surface area ²	m ² ·g ⁻¹	1.21	0.73	1.62
Slake durability ³	%	35.3	34.2	33.5
S	wt %	0.02	0.02	0.18
Sulfide	wt %	0.03	0.03	0.16
SO ₄	wt %	<0.4	0.01	0.02
C	wt %	0.05	0.03	0.03
Carbonate	wt %	0.06	0.03	0.04
SiO ₂	wt %	67.6	67.8	66.5
Al ₂ O ₃	wt %	15.8	15.6	16.3
Fe ₂ O ₃	wt %	3.9	4.0	4.2
MgO	wt %	1.3	1.6	1.6
CaO	wt %	0.7	0.8	0.9
K ₂ O	wt %	5.5	5.2	4.7
MnO	wt %	0.06	0.04	0.04
Paste pH		8.36	8.26	7.8
NP	kg CaCO ₃ t ⁻¹	9.32	9.17	9.34
AP	kg CaCO ₃ t ⁻¹	0.41	0.65	4.91
Net NP	kg CaCO ₃ t ⁻¹	8.9	8.53	4.42
NP/AP	ratio	22.7	14.1	2.1
NAG	kg H ₂ SO ₄ t ⁻¹	0.08	0.49	4.50

Notes: ¹ S content—Type I < 0.04 wt %, Type II = 0.04 to 0.08 wt %, Type III > 0.08 wt %; ² Mean surface area calculated by the BET method [29]; ³ Slake durability index lists material in the range of 0%–25% as very low, 25%–50% as low, 50%–75% as medium, 75%–90% as high, 90%–95% as very high, and 95%–100% as extremely high for material to resist weathering and abrasion.

Figure 2. Temporal variation (moving average trendline of a 10-data point window) of the specific conductance of leachate from warm and cold humidity cells and specific conductance ratio of warm and cold Type III waste rock leachate.

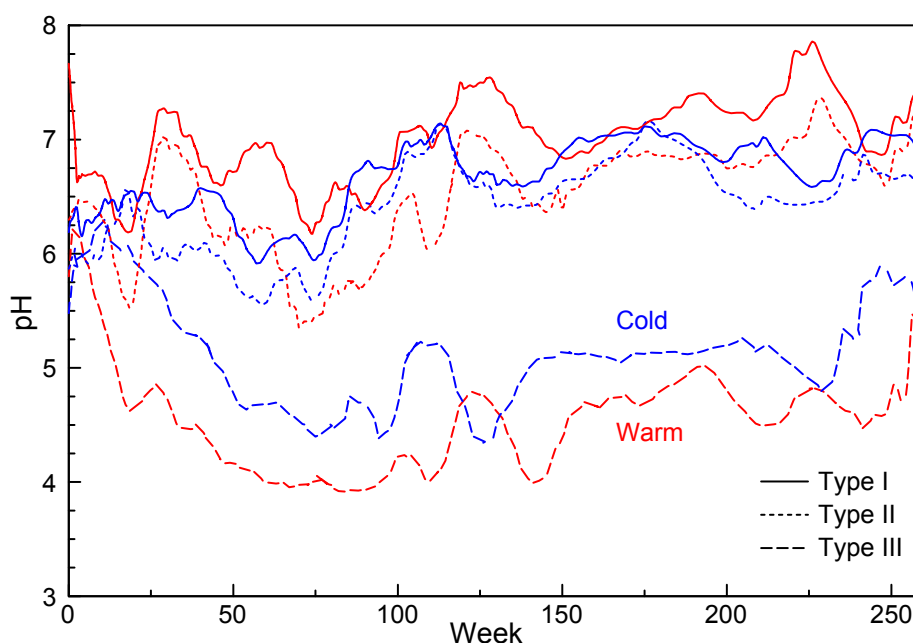


Acid neutralization by carbonates in Type III rock was expected to be short in duration due to the relatively higher sulfide content of the rock (0.16 wt %, Table 1) and its low carbonate content (0.04 wt %). Following carbonate depletion, the primary acid-neutralizing mechanisms typically are the dissolution of Al and Fe hydroxides and reactive aluminosilicate minerals [15]. Dissolution of Fe hydroxides provides little neutralizing capacity in a pH environment greater than 4 [43]. The pH of the Type III warm and cold leachate reflected such a sequence of acid neutralization reactions (Figure 3). The pH declined in the Type III cells because the carbonate content was not sufficient to neutralize all the acid generated from sulfide oxidation, and the pH decreased rapidly until it stabilized in the 4–4.5 range. Following a period of relatively stable pH (between weeks 50 and 100), acid generation appeared to weaken as pH rose to the 4.5–5 range in the Type III warm and cold cells (Figure 3). Type I and II rock also produced initial large releases of dissolved solids (Figure 2), but neither produced a declining pH environment similar to the Type III rock (Figure 3). The lack of a substantial decline in pH for the Type I and II leachate is indicative of the smaller sulfide content and sufficient acid neutralization by carbonate minerals to maintain a near-neutral pH. Results from the Type II cells indicate a relatively small decrease in pH (minimum of 5.5) from weeks 25 to 75, which is still within the acid neutralization range for carbonate minerals.

Results from the Type III cold cells indicate a lower weathering rate (Figure 2) and more limited changes in pH (Figure 3) compared to the warm cells. Warm and cold Type III data show a decrease in pH, but the decrease was delayed and more gradual in the cold cells because of the influence of temperature on reaction rates. The temperature dependence of sulfide oxidation rates can be described by the Arrhenius equation [44], and bacterial abundance and their catalysis of oxidation reactions typically decrease at lower temperatures [45,46]. The difference in reactions rates due to temperature can be examined using specific conductance values as estimates of chemical weathering rates

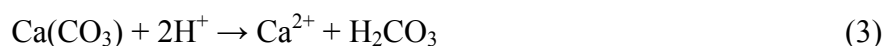
(assuming a lack of physical weathering after the initial flushing that removed products attributed to physical weathering because of mining). The ratio of the Type III warm and cold specific conductance (Figure 2) indicates much stronger weathering initially in the warm cells, which is driven by faster reaction rates. By the 75th week, weathering in the warm and cold Type III cells produced a relatively constant specific-conductance ratio near 1.5. This steady ratio is evidence of the primary effect of temperature on reactions rates, and a loss of other influences such as bacterial catalysis of the reactions.

Figure 3. Temporal variation (moving average trendline of a 5-data point window) of the pH of leachate from the warm and cold humidity cells.



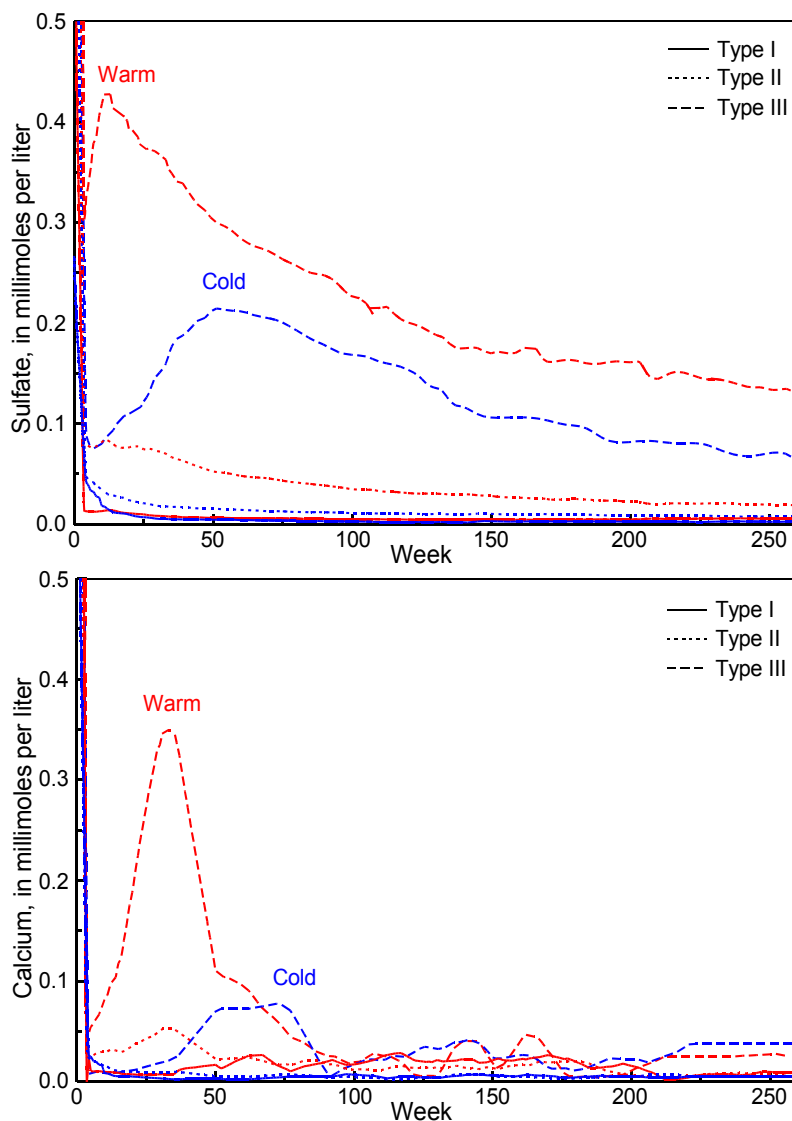
4.3. Sulfide Oxidation and Acid Neutralization by Carbonate Minerals

The assumptions that SO_4 is derived from sulfide oxidation and that Ca is released during carbonate dissolution are reasonable given the absence of other groups of S- or Ca-bearing minerals. Calcite is the primary carbonate (random dispersion of grains similar in size to pyrrhotite) with only minor traces of Mg in the calcite and very little dolomite [$\text{CaMg}(\text{CO}_3)_2$] found in the granite [21]. Carbonates such as magnesite [MgCO_3], ankerite [$\text{Ca}(\text{Mg,Fe})(\text{CO}_3)_2$], and siderite [FeCO_3] have not been found in Diavik waste rock [21], although such minerals may form as secondary minerals in pore waters with weathering [3]. Dissolution of calcite (Equation (3)) is a near 1:1 acid neutralization reaction with acid generated from pyrrhotite oxidation (Equation (1)).



The limited amount of sulfide in the Type I and II rock produced relatively small releases of Ca and SO_4 compared to those from the Type III rock (Figure 4). Acid generated from sulfide oxidation in Type III rock produced increasing SO_4 and Ca concentrations that peaked between 10 and 75 weeks, with releases from the warm cells peaking earlier than releases from the cold cells. Weathering of the rock in the cold cells also resulted in lower concentrations of SO_4 and Ca due to decreased rates of sulfide oxidation at the lower temperature (Figure 4).

Figure 4. Temporal variation (moving average trendline of a 7-data point window) of SO_4 and Ca in leachate from warm and cold humidity cells.



Acid-generation/neutralization relations can be examined through a comparison of sulfide oxidation products (primarily SO_4) and acid neutralization products (such as Ca from carbonates) [47]. To visualize the change in the relations, the release of SO_4 and Ca and associated load accumulations were compared for time intervals of weeks 0–25, 25–50, 50–100, 100–125, 125–150, 150–200, and 200–250, when variation in pH suggest changes in acid generation or acid neutralization (Figure 5). Type I rock contained available carbonate minerals to neutralize the small amount of acid generated through the oxidation of the limited sulfide minerals throughout the experiment, except for the 25–50 week period. No substantial decrease in pH corresponded to the 25–50 week period (Figure 3). The acid generation-neutralization relations for the Type II cells (Figure 5) indicate insufficient carbonate content for acid neutralization, which is reflected in the lower pH values for Type II cells compared to Type I cells during the first 100 weeks of the experiment (Figure 3). The oxidation of the larger mass of sulfide minerals in Type III rock overwhelmed the carbonate acid-neutralization capacity during the first 25 weeks (Figure 3) and resulted in a substantially greater release of SO_4 compared to Ca (Figure 5). The differences in acid generation-neutralization relations (Figure 5) can be correlated to the sulfide

and carbonate content of the Type I and Type III rock types (Table 1). However, the Type II rock appears to contain more sulfide than indicated by acid-base accounting estimates (Table 1). Such underestimation of sulfide content and potential acid generation is a common issue with static tests, particularly in low sulfide rocks where there is greater uncertainty with such short-term analyses [38]. A comparison of SO₄ loads and acid generation-neutralization relations indicates that the Type II rock likely contained 0.05–0.06 wt % S, which is within the content estimated by Diavik screening procedures (0.04–0.08 wt %).

4.4. Sulfide Reaction Activation Energy

To further evaluate the effect of temperature and changes on the microbially-mediated oxidation of sulfide, the activation energy of the warm and cold cell reaction rates of sulfide oxidation were calculated using the Arrhenius equation (Equation (4)).

$$E_a = \frac{(RT_1T_2)}{T_1 - T_2} \ln \frac{k_1}{k_2} \quad (4)$$

where E_a is the activation energy (kJ·mol⁻¹), R is the universal gas constant (8.314 × 10⁻³ kJ·mol⁻¹·K⁻¹), and T_1 and T_2 are temperatures (K) at the respective times of the observed rate constants (k_1 and k_2 in mol·m⁻²·s⁻¹). Pyrrhotite grains in the schist typically range from 50 to 200 μm [21]. Janzen *et al.* [18] found the surface area of pyrrhotite with grain diameters between 125 and 180 μm to range from 0.17 to 2.1 m²·g⁻¹; the larger surface areas were attributed to fractures, similar to those observed in Diavik pyrrhotite (Figure 6). Given the possible fractured nature of the pyrrhotite and an estimated median grain size near 125 μm, a surface area of 1 m²·g⁻¹ was selected for calculating the oxidation rate based on SO₄ discharged from the humidity cells. The total surface area available was adjusted according to the total mass available for weathering as calculated from the wt % S (Table 1) and a reduced total mass available each week by subtracting the accumulated S discharged from each cell.

The variation in activation energy of sulfide oxidation for the various rock types correlates with anticipated changes in likely sulfide availability (Figure 7). The largest concentrations of SO₄ in leachate from the Type I and III humidity cells occurred during a decline in activation energy when sulfide availability was the greatest and oxidizing bacteria likely were available to catalyze the reaction; oxygen and sulfide availability promote bacterial growth and activity, which will accelerate the oxidation reaction and production of SO₄ [3]. Excluding the first part of the experiment, which was influenced by the flushing of initial SO₄ formed during mining, a maximum oxidation rate of 7.7 × 10⁻¹⁰ mol·m⁻²·s⁻¹ was observed in week 11 from the warm Type III cells, and a maximum rate of 3.5 × 10⁻¹⁰ mol·m⁻²·s⁻¹ was observed during week 44 for the cold Type III cells. These rates are similar to rates observed by Nicholson and Schärer [48] and Janzen *et al.* [18] for pyrrhotite oxidation. The smallest activation energies were coincident with the lowest pH conditions (Figures 3 and 7). The low pH of the leachate is a result of the sulfide oxidation reaction and cannot be viewed as a cause. However, low pH conditions can be considered an augmenting influence on continued oxidation due to the enhanced weathering and solubility of Fe³⁺—an important oxidant of pyrrhotite [3]. The decrease in activation energy (increase in pH) for all rock types near the end of the experiment is a result of depletion of available sulfide, which produces similar release rates for warm and cold conditions.

Figure 5. Acid generation-neutralization relations for cumulative loads of Ca and SO₄ leached from warm and cold humidity cells during intervals of weeks 0–25, 25–50, 50–100, 100–125, 125–150, 150–200, and 200–250. Week intervals above the neutralization-acidification line indicate continued stable pH conditions (neutralization), and intervals below the line indicate possible decreasing or continued acidic pH conditions (acid generating). Select intervals are highlighted to indicate periods of early or greatest acidification. The Ca and SO₄ relations were extended for all intervals to present the acid generation-neutralization relations on a similar scale (not dependent on load amount).

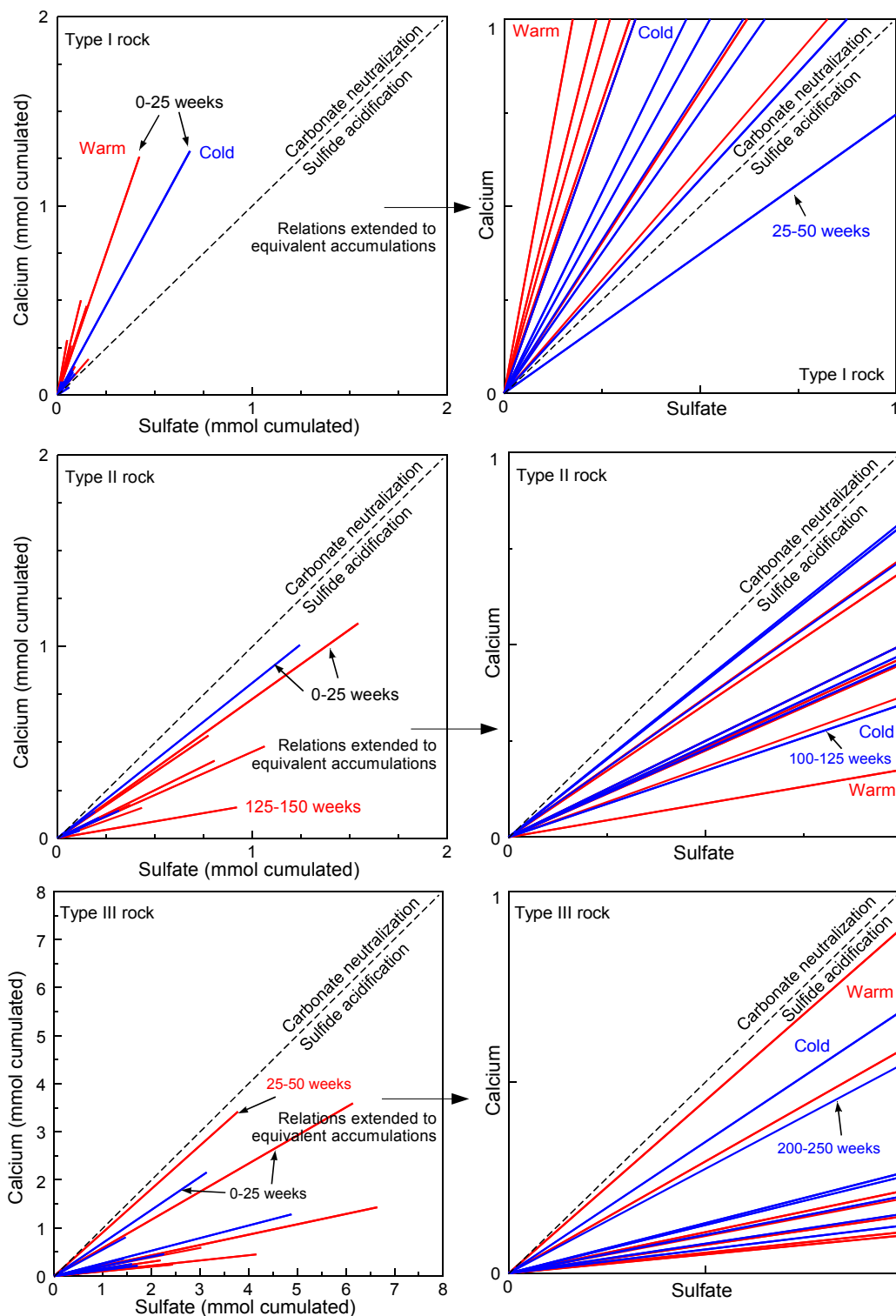


Figure 6. Example of a fractured pyrrhotite grain in waste rock from the Diavik mining site.

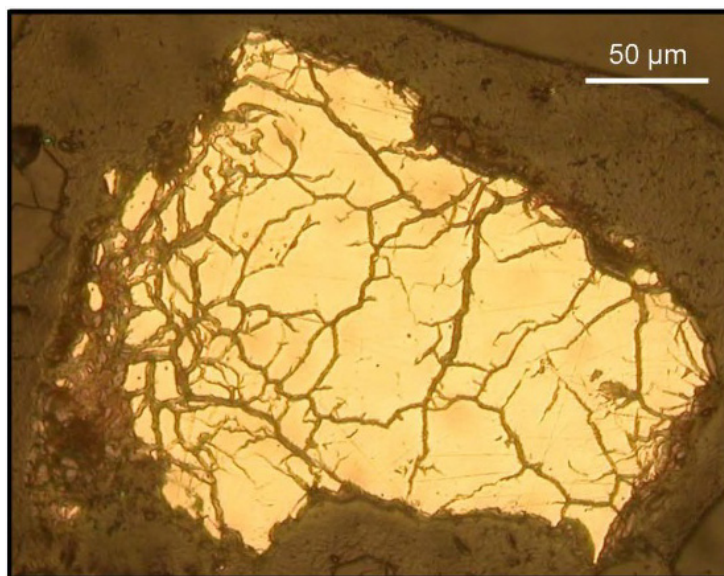
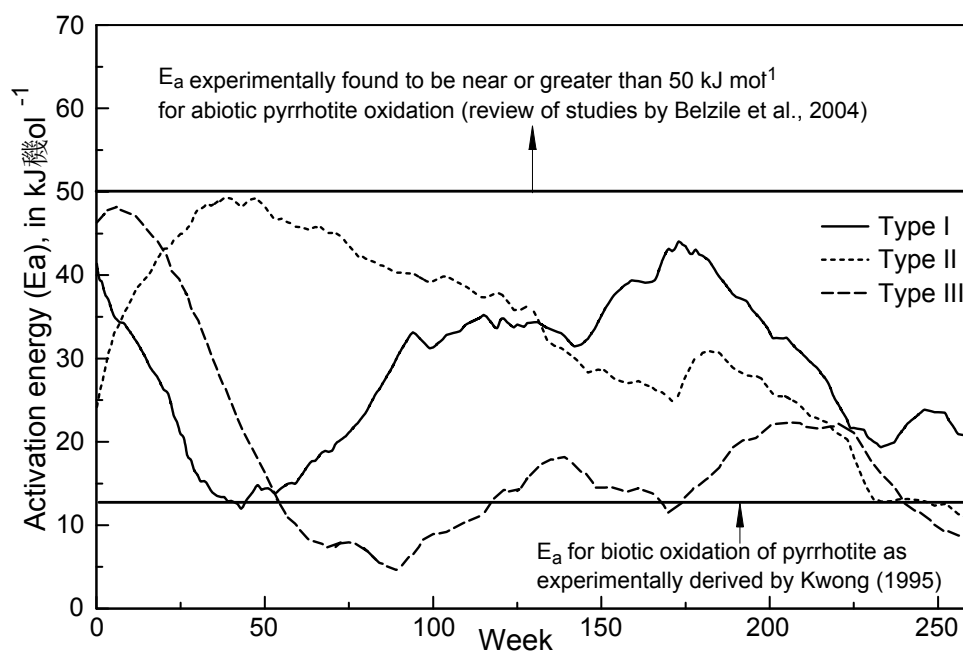


Figure 7. Activation energy of sulfide oxidation in Diavik waste rock calculated from the SO_4 concentration in leachate from the warm and cold humidity cells.



All rock samples contained large amounts of neutrophilic, S-oxidizing bacteria (10^2 to 10^7 colony forming units (viable bacteria) per gram for four samples of each rock type); very small amounts of acidophilic, S-oxidizing bacteria for each rock type (<25 colony forming units per gram); and no detectable colony forming units of acidophilic, Fe-oxidizing bacteria. Blowes *et al.* [49] indicated that neutrophilic bacteria, such as *Thiobacillus*, typically are the initial oxidizing bacteria. With the formation of acidic conditions, acidophilic species such as *Acidithiobacillus thiooxidans* and *Acidithiobacillus ferrooxidans* promote additional oxidation and effectively catalyze the reaction [3]. As the humidity-cell experiment proceeded beyond the period of greatest sulfide oxidation, bacterial populations likely decreased along with readily available sulfide for oxidation, which resulted in

decreasing oxidation rates and increasing activation energies after 50 weeks for the Type I rock and 90 weeks for the Type III rock (Figure 7). Activation energies for the oxidation of sulfide in the Type II rock did not conform to the expected early decrease but instead increased until week 50 and then gradually decreased over the remainder of the experiment (Figure 7). This unusual activation energy profile and the underestimation of the sulfide content by static tests indicate a lack of readily available sulfide during the initial stage of the experiment. The Type II acid generation-neutralization relation (Figure 5) and activation energy trend (Figure 7) can be explained by the presence of more sulfide than determined from static tests (Table 1), but this sulfide appears to be less readily available (e.g., greater inhibition by encapsulation, secondary minerals, or further oxidized minerals) compared to that present in the Type I and III rocks.

4.5. Sulfide Oxidation and Acid Consumption by Al-Bearing Minerals

The non-carbonate assemblage in the Diavik waste rock predominantly consists of minerals present in the granite (K-feldspar, albite, and quartz) and biotite schist (quartz, albite, and biotite) [21]. With a depletion of the acid neutralization capacity by carbonate minerals, Al-bearing phases—such as $\text{Al}(\text{OH})_3$ —contribute to acid neutralization (Equation (5)) and pH may stabilize in the 4 to 5 range [3,38].

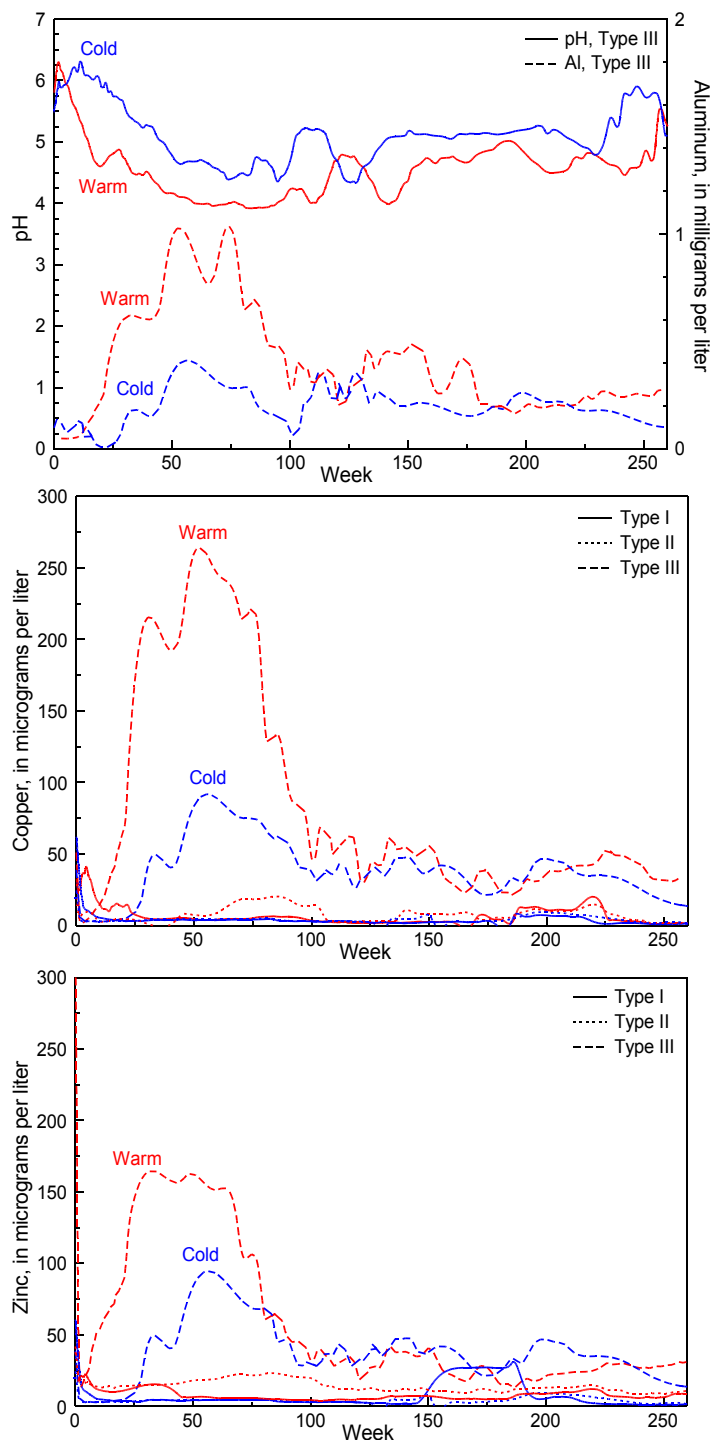


The relatively stable pH (near 4) for the Type III leachate between weeks 50 and 100 (Figure 3) and the increase in dissolved Al concentrations (Figure 8) indicate a chemical weathering pattern of sulfide oxidation and acid neutralization by Al-bearing minerals. The rates of Al release varied according to pH because the dissolution of Al-bearing phases is favored at low pH and H^+ competes with such metals for sorption sites. Acid neutralization by Al-bearing phases will occur with the release of Al^{3+} from more easily weathered minerals such as biotite. Dissolution of aluminosilicates likely will follow a predicted order based on the point of zero charge of the minerals [3], although release rates may decline with element depletion in the reacting layer and rates can approach those of the slowest dissolving ion [50]. The weathering of pyrrhotite and biotite in the schist produced a visible secondary mineral phase (ocherous precipitate) in the Type III cells after the pH dropped below 4.5, although this precipitate dissolved at a later date. The precipitate likely was jarosite ($[\text{KFe}_3(\text{SO}_4)_2(\text{OH})_6]$; Equation (6)), which is indicative of the dissolution of biotite (K and additional Fe source), Fe^{2+} to Fe^{3+} oxidation, and an acidic environment [6,51–55]. Formation of jarosite is an indication of incongruent dissolution of biotite (release of more easily removed elements such as K). A pH of near 3 is necessary for congruent dissolution [56].



The loss of SO_4 to secondary mineral precipitation is possible (e.g., through the formation of jarosite), but is not expected to be significant. Substantial losses typically occur with more easily formed minerals such as gypsum $[\text{CaSO}_4 \cdot 2\text{H}_2\text{O}]$, but saturation indices calculated using PHREEQC (U.S. Geological Survey, Denver, CO, USA) indicate that the leachate was undersaturated with respect to gypsum throughout experiment.

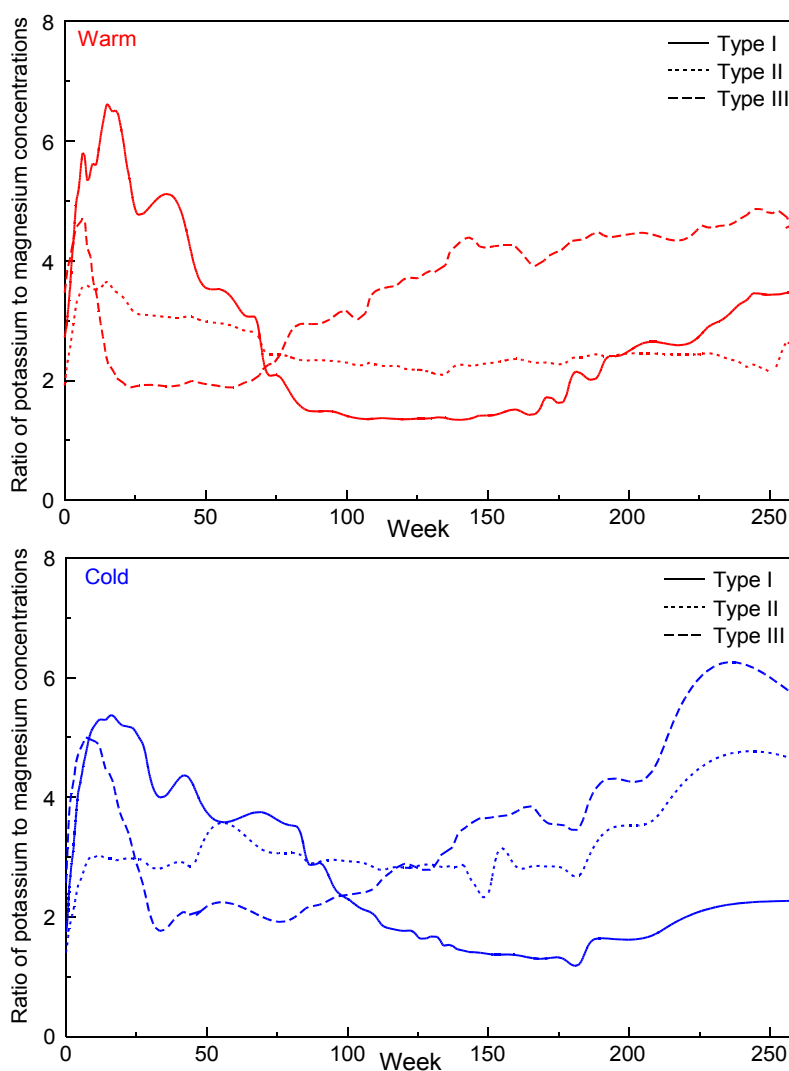
Figure 8. Temporal variation (moving average trendline of a 3-data point window) of pH and Al in leachate from warm and cold humidity cells containing Type III waste rock, and Cu and Zn in leachate from warm and cold humidity cells containing Type I, II, and III waste rock.



Acid neutralization by biotite, compared to other aluminosilicates such as K-feldspar, can be examined through a comparison of the release of K and Mg. Both elements are found in biotite, but the elements differ in their crystal location (octahedral sheet compared to the tetrahedral sheet) and bonding environment (monovalent compared to divalent). Potassium is an inter-sheet, weakly-bonded ion that can release into solution at a rate two orders of magnitude greater than Mg during initial and

extended weathering [50]. Minor additional sources of Mg include spinel [MgAl_2O_4], but K is found in greater quantities in the K-feldspar compared to the biotite [21]. A change in the ratio of K/Mg that corresponds to changes in pH reflects changes in mineral source and their reactivity. The K/Mg ratio in leachate from the Type I cells (warm and cold) indicates larger initial ratios with weathering due to the contribution of K from the more easily weathered biotite with correspondingly smaller contributions of Mg (Figure 9). The ratios for the Type II and III rock indicate less pronounced initial peaks and reduced ratios indicating more extensive weathering of the biotite due to greater releases of Mg with increased acidity. Following the lower pH period (after 100 weeks), the K/Mg ratios either stabilized or began to increase. Increasing ratios during this period can be attributed to release of K from the more weathering-resistant but larger K source in the K-feldspar. This K contribution is reflected in the different starting periods of the ratio increase for the Type I and III cells (Figure 9); the increase in K concentrations began substantially earlier (75 to 100 weeks) in the Type III cells than in the Type I cells (about 175 weeks). The increased acidity for the Type III leachate would allow for increased weathering of other aluminosilicates, such as the K-feldspar, as the K release slowed in the biotite because of depletion of K in the reactive layers.

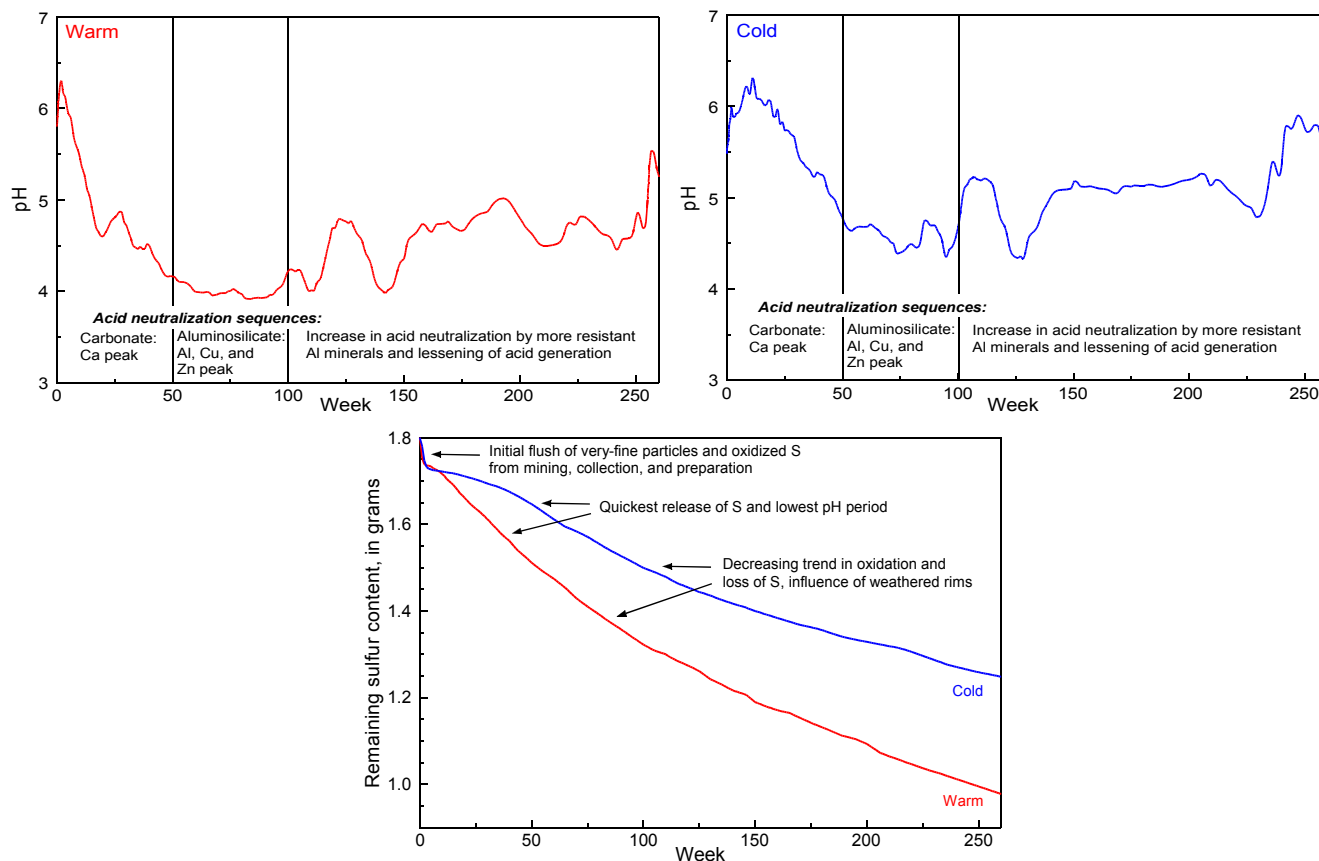
Figure 9. Ratio of K and Mg concentrations (moving average trendline of a 10-data point window) in leachate from warm and cold humidity cells.



4.6. Sulfide Availability, Acid Neutralization Sequences, and the Temperature Effect

Changes in acid generation and neutralization in leachate from the Diavik waste rock are evident in the pH trends of the Type III leachate, which can be combined with changes in element release rates to evaluate the effect of temperature, sulfide availability, and acid neutralization sequences (Figure 10). The lower pH during the first year of the experiment in the warm cells (Figure 10) correspond to larger concentrations of Al, Cu, and Zn in solution (Figure 8). The warmer temperature has a compounding effect of increasing chemical reactions and bacteria activity, which results in substantially greater weathering rates (Figures 2 and 10). The moderating influence on weathering at the colder temperature is evident in the less pronounced and shorter duration of lower pH and smaller element release rates (Figure 10).

Figure 10. Temporal variation (moving average trendline of a 3-data point window) of the pH of leachate and consumption of sulfide minerals (as S) through weathering and leaching from Type III rock in warm and cold humidity cells.



With this low-sulfide granitic waste rock, acid generation was expected to decline during the experiment due to sulfide depletion and decreased sulfide availability with the formation of weathered rims. Pyrrhotite oxidation can result in partial oxidation and dissolution where continued weathering of the sulfide is influenced by the coverage and depth of the alteration front that is composed of weathered rims around the sulfide core [35]. This phenomenon produces polysulfides, other Fe-sulfides, elemental S, and various Fe (oxyhydr)oxides in the weathered rims [18,57,58]. A lessening of sulfide oxidation and acid generation is evident near 100 weeks in the warm and cold

Type III cells, as indicated by an increase in pH (Figure 10), which corresponds to the decline in metal release and solubility (Figure 8). Ahonen and Tuovinen [45] suggested that because of the lower activation energy of microbially-mediated oxidation of pyrrhotite compared to other Fe sulfides, the rate-limiting factor is diffusion of reactants and products in weathering pyrrhotite. The decrease in oxidation is the product of rate-limiting weathered rims, which decrease the flux of oxygen to the sulfide and release of oxidation products [59,60]. The lessening of sulfide oxidation and acid generation continued until the end of the experiment in the warm and cold cells, even though more than half of the initial S content was still present in the Type III waste rock by the end of the fifth year of the experiment (Figure 10). The formation of weathered rims appears to be a strong limiting factor in weathering of sulfides in Diavik waste rock under warm and cold conditions.

5. Summary and Conclusions

Weathering characteristics of Diavik waste rock were evaluated according to the physical characteristics of the rock and the temporal variation of leachate chemistry from this long-term, humidity-cell experiment. The weathering of sulfide in Diavik waste rock produces substantially different aqueous geochemical conditions and element release rates depending on which of the prescribed waste rock types—I (<0.4 wt % S), II (0.4 to 0.8 wt % S), or III (>0.8 wt % S)—is present. The relatively small concentrations of sulfide in these samples of Type I and Type II rock were insufficient to overcome the similarly small acid-consumption capacity of the calcite. Type III rock has the potential to generate sufficient acid to relatively quickly deplete the available carbonate content and decrease the leachate pH to less than 5. The release of acid and metals from the sulfide minerals—primarily pyrrhotite with traces of pyrite, chalcopyrite, and sphalerite—produces elevated concentrations of Cu and Zn in solution. The decline in carbonate minerals is followed by acid neutralization by Al-bearing mineral dissolution that can maintain the pH above 4. The weathering of the Al-bearing minerals and acidic conditions releases Al into solution along with other metals. The relatively low concentration of sulfide in Type III waste rock limits the period of low pH as observed during the latter half of the experiment. Acid generation peaked within the first two years of the experiment (earliest for the warm cells), but sulfide oxidation and acid generation associated with Type III rock likely could continue for years as indicated by the slow recovery of the pH environment.

All results from the humidity-cell experiment indicate the strong influence of temperature on acid generation and neutralization. The reduced reaction rates in the cold cells are attributed to the influence of temperature on reaction rates and reduced bacteria presence and (or) activity for catalysis of the oxidation reaction. With weathering, reduction of available reactive surface areas increased the activation energy required for oxidation. Following carbonate depletion, release of SO₄ and other weathering products from Type III rock produced warm to cold cell ratios near 1.5 for SO₄ (typically between 1 and 2) and specific conductance (Figure 2), where they remained until the end of the experiment. These release rates indicate that temperature was the primary influence on oxidation reactions during this period, which followed the more active oxidation period defined by a low pH, large element releases, and a decline in activation energy of the oxidation reaction.

A long-term assessment of acid generation-neutralization relations in Diavik waste rock needs to consider changes in mineral content and availability, acid neutralization sequences, and the variable

element release rates associated with sequential stages of sulfide oxidation. The evolution of the oxidation rates used for calculation of the activation energy of sulfide oxidation will be used to evaluate field-site sulfide weathering and changes in the geochemical environment. Secondary minerals can affect sulfide oxidation rates as indicated by the decrease in acid generation attributed to the formation of sulfide weathered rims even though a significant portion of the total sulfide content remained. Direct correlation of the results of the 5-year, humidity-cell experiment, such as element concentrations, to the field site may be difficult because the controlled environment and regular introduction and saturation with water are very different from field conditions. However, changes in pH, specific conductance, and relative element release rates in leachate from the Type III waste rock can be viewed as distinct acid-consuming sequences that reflect alteration of mineral content from weathering, which should correlate to similar changes in field-site leachate characteristics.

Acknowledgments

The cooperation of many individuals and organizations was essential for completion of this study. Funding for this research was provided by a Collaborative Research and Development Grant from the Natural Sciences and Engineering Research Council of Canada awarded to David W. Blowes, Principal Investigator; Diavik Diamond Mines, Inc.; an Innovation Fund Award from the Canada Foundation for Innovation awarded to James F. Barker, Principal Investigator; the International Network for Acid Prevention; and the Mine Environment Neutral Drainage Program.

Author Contributions

Jeff B. Langman, Mandy L. Moore, Carol J. Ptacek, and David W. Blowes completed the work described in Section 3. All authors contributed to the preparation and writing of the manuscript.

Conflicts of Interest

The authors declare no conflict of interest.

References

1. Nordstrom, D.K.; Southam, G. Geomicrobiology of sulfide mineral oxidation. *Rev. Mineral. Geochem.* **1997**, *35*, 361–390.
2. Nordstrom, D.K.; Alpers, C.N. Geochemistry of Acid Mine Waters. In *the Environmental Geochemistry of Mineral Deposits*; Plumlee, G.S., Logsdon, M.J., Eds.; Society of Economic Geologists: Littleton, CO, USA, 1999; pp. 133–160.
3. Blowes, D.W.; Ptacek, C.J.; Jambor, J.L.; Weisener, C.G. The Geochemistry of Acid Mine Drainage. In *Environmental Geochemistry*; Lollar, B.S., Ed.; Elsevier-Pergamon: Oxford, UK, 2003; pp. 149–204.
4. Blowes, D.W.; Jambor, J.L.; Appleyard, E.C.; Reardon, E.J.; Cherry, J.A. Temporal observations of the geochemistry and mineralogy of a sulfide-rich mine-tailings impoundment, Heath Steele Mines, New Brunswick. *Explor. Min. Geol.* **1992**, *1*, 251–264.

5. Pyatt, F.B.; Grattan, J.P. Some consequences of ancient mining activities on the health of ancient and modern human populations. *J. Public Health* **2001**, *23*, 235–236.
6. Moncur, M.C.; Ptacek, C.J.; Blowes, D.W.; Jambor, J.L. Release, transport and attenuation of metals from an old tailings impoundment. *Appl. Geochem.* **2005**, *20*, 639–659.
7. Sapsford, D.J. Humidity cell tests for the prediction of acid rock drainage. *Miner. Eng.* **2009**, *22*, 25–36.
8. Bowell, R.J.; Williams, K.P.; Connelly, R.J.; Sadler, P.J.K.; Dodds, J.E. Chemical Containment of Mine Waste. In *Chemical Containment of Waste in the Geosphere*; Geological Society Special Publication; Metcalfe, R., Rochelle, C.A., Eds.; Geological Society of London: London, UK, 1999; Volume 157, pp. 213–240.
9. Malmström, M.E.; Destouni, G.; Banwart, S.A.; Strömberg, B.H.E. Resolving the scale-dependence of mineral weathering rates. *Environ. Sci. Technol.* **2000**, *34*, 1375–1378.
10. Lefebvre, R.; Hockley, D.; Smolensky, J.; Gélinas, P. Multiphase transfer processes in waste rock piles producing acid mine drainage 1: Conceptual model and system characterization. *J. Contam. Hydrol.* **2001**, *52*, 137–164.
11. Bowell, R.J. The Hydrogeochemical Dynamics of Mine Pit Lakes. In *Mine Water Hydrogeology and Geochemistry*; Geological Society Special Publication; Younger, P.L., Ed.; Geological Society of London: London, UK, 2002; Volume 198, pp. 159–185.
12. Strömberg, B.; Banwart, S.A. Experimental study of acidity-consuming processes in mining waste rock: Some influences of mineralogy and particle size. *Appl. Geochem.* **1999**, *14*, 1–16.
13. Stockwell, J.; Smith, L.; Jambor, J.L.; Beckie, R. The relationship between fluid flow and mineral weathering in heterogeneous unsaturated porous media: A physical and geochemical characterization of a waste-rock pile. *Appl. Geochem.* **2006**, *21*, 1347–1361.
14. Morgan, B.; Lahav, O. The effect of pH on the kinetics of spontaneous Fe(II) oxidation by O₂ in aqueous solution—Basic principles and a simple heuristic description. *Chemosphere* **2007**, *68*, 2080–2084.
15. Jurjovec, J.; Ptacek, C.J.; Blowes, D.W. Acid neutralization mechanisms and metal release in mine tailings: A laboratory column experiment. *Geochim. Cosmochim. Acta* **2002**, *66*, 1511–1523.
16. Gunsinger, M.R.; Ptacek, C.J.; Blowes, D.W.; Jambor, J.L.; Moncur, M.C. Mechanisms controlling acid neutralization and metal mobility within a Ni-rich tailings impoundment. *Appl. Geochem.* **2006**, *21*, 1301–1321.
17. Arvidson, R.S.; Ertan, I.E.; Amonette, J.E.; Luttge, A. Variation in calcite dissolution rates: A fundamental problem? *Geochim. Cosmochim. Acta* **2003**, *67*, 1623–1634.
18. Janzen, M.P.; Nicholson, R.V.; Scharer, J.M. Pyrrhotite reaction kinetics: Reaction rates for oxidation by oxygen, ferric iron, and for nonoxidative dissolution. *Geochim. Cosmochim. Acta* **2000**, *64*, 1511–1522.
19. Environment Canada. Climate: Historical Climate Data. Available online: http://climate.weather.gc.ca/index_e.html (accessed on 23 June 2013).
20. Blowes, D.W.; Logsdon, M.J. *Diavik Geochemistry Baseline Report*; Canadian Environmental Assessment Agency: Ottawa, ON, Canada, 1998.
21. Jambor, J.L. *Mineralogy of the Diavik Lac de Gras Kimberlites and Host Rocks*; Canadian Environmental Assessment Agency: Ottawa, ON, Canada, 1997.

22. American Society for Testing and Materials. *Standard Practice for Sampling Aggregates*; American Society for Testing and Materials (ASTM) International: West Conshohocken, PA, USA, 2003.
23. American Society for Testing and Materials. *Standard Practice for Reducing Samples of Aggregate to Testing Size*; American Society for Testing and Materials (ASTM) International: West Conshohocken, PA, USA, 2003.
24. American Society for Testing and Materials. *Standard Practice for Probability Sampling of Materials*; American Society for Testing and Materials (ASTM) International: West Conshohocken, PA, USA, 1996.
25. American Society for Testing and Materials. *Standard Practice for Dry Preparation of Soil Samples for Particle-Size Analysis and Determination of Soil Constants*; American Society for Testing and Materials (ASTM) International: West Conshohocken, PA, USA, 2002.
26. Smith, R.M.; Grube, W.E.; Arkle, T.; Sobek, A. *Mine Spoil Potentials for Soil and Water Quality*; U.S. Environmental Protection Agency: Washington, DC, USA, 1974.
27. Sobek, A.A.; Schuller, W.A.; Freeman, J.R.; Smith, R.M. *Field and Laboratory Methods Applicable to Overburdens and Mine Soils*; U.S. Environmental Protection Agency: Washington, DC, USA, 1978.
28. Lawrence, R.W.; Wang, Y. Determination of Neutralization Potential in the Prediction of Acid Rock Drainage. In Proceedings of the 4th International Conference on Acid Rock Drainage, Vancouver, BC, Canada, 30 May–6 June 1997.
29. Brunauer, S.; Emmett, P.H.; Teller, E. Adsorption of gases in multimolecular layers. *J. Am. Chem. Soc.* **1938**, *60*, 309–319.
30. American Society for Testing and Materials. *Test Method for Slake Durability of Shales and Similar Weak Rocks*; American Society for Testing and Materials (ASTM) International: West Conshohocken, PA, USA, 2004.
31. Cochran, W.G. Estimation of bacterial densities by means of the “most probable number”. *Biometrics* **1950**, *6*, 105–116.
32. Benner, S.G.; Gould, W.D.; Blowes, D.W. Microbial populations associated with the generation and treatment of acid mine drainage. *Chem. Geol.* **2000**, *169*, 435–448.
33. Scharer, J.M.; Bolduc, L.; Phillips, H.A.; Pettit, C.M.; Kwong, E.C.M. *Review of Measurement Techniques to Support the Application of Biotechnology for the Abatement of Acid Mine Drainage*; Mining and the Environment II; Laurentian University, Centre in Mining and Mineral Exploration Research: Sudbury, ON, USA, 1999; pp. 1163–1172.
34. American Society for Testing and Materials. *Test Method for Laboratory Weathering of Solid Materials Using a Humidity Cell*; American Society for Testing and Materials (ASTM) International: West Conshohocken, PA, USA, 1996.
35. Jambor, J.L.; Dutrizac, J.E.; Chen, T.T. Contribution of Specific Minerals to the Neutralization Potential in Static Tests. In Proceedings of Fifth International Conference on Acid Rock Drainage; Society for Mining, Metallurgy, and Exploration: Littleton, CO, USA, 2000; pp. 551–565.
36. Jambor, J.L.; Dutrizac, J.E.; Groat, L.A.; Raudsepp, M. Static tests of neutralization potentials of silicate and aluminosilicate minerals. *Environ. Geol.* **2002**, *43*, 1–17.
37. Jambor, J.L.; Dutrizac, J.E.; Raudsepp, M. Measured and computed neutralization potentials from static tests of diverse rock types. *Environ. Geol.* **2007**, *52*, 1019–1031.

38. Price, W.A. *Prediction Manual for Drainage Chemistry from Sulphidic Geological Materials*; CANMET-Mining and Mineral Sciences Laboratories: Smithers, BC, Canada, 2009.
39. Furrer, G.; Stumm, W. The coordination chemistry of weathering: I. Dissolution kinetics of δ - Al_2O_3 and BeO. *Geochim. Cosmochim. Acta* **1986**, *50*, 1847–1860.
40. Schott, J.; Berner, R.A.; Sjöberg, E.L. Mechanism of pyroxene and amphibole weathering—I. Experimental studies of iron-free minerals. *Geochim. Cosmochim. Acta* **1981**, *45*, 2123–2135.
41. Wehrli, B. Monte Carlo simulations of surface morphologies during mineral dissolution. *J. Colloid Interface Sci.* **1989**, *132*, 230–242.
42. Lapakko, K.A.; White, W.W. Modification of the ASTM 5744-96 Kinetic Test. In Proceedings of Fifth International Conference on Acid Rock Drainage; Society for Mining, Metallurgy, and Exploration: Littleton, CO, USA, 2000; pp. 631–639.
43. Merkel, B.J.; Planer-Friedrich, B. Theoretical background. In *Groundwater Geochemistry*; Nordstrom, D.K., Ed.; Springer: Berlin, Germany, 2008; pp. 1–68.
44. Nicholson, R.V.; Gillham, R.W.; Reardon, E.J. Pyrite oxidation in carbonate-buffered solution: 1. Experimental kinetics. *Geochim. Cosmochim. Acta* **1988**, *52*, 1077–1085.
45. Ahonen, L.; Tuovinen, O.H. Bacterial oxidation of sulfide minerals in column leaching experiments at suboptimal temperatures. *Appl. Environ. Microbiol.* **1992**, *58*, 600–606.
46. Dawson, R.F.; Morin, K.A. *Acid Mine Drainage in Permafrost Regions Issues, Control Strategies and Research Requirements*; CANMET, Mine Environment Neutral Drainage, and Department of Indian and Northern Affairs: Ottawa, ON, Canada, 1996.
47. Benzaazoua, M.; Bussière, B.; Dagenais, A.M.; Archambault, M. Kinetic tests comparison and interpretation for prediction of the Joutel tailings acid generation potential. *Environ. Geol.* **2004**, *46*, 1086–1101.
48. Nicholson, R.V.; Scharer, J.M. Laboratory Studies of Pyrrhotite Oxidation Kinetics. In *Environmental Geochemistry of Sulfide Oxidation*; ACS Symposium Series; Alpers, C.N., Blowes, D.W., Eds.; American Chemical Society: Washington, DC, USA, 1994; Volume 550, pp. 14–30.
49. Blowes, D.W.; Al, T.; Lortie, L.; Gould, W.D.; Jambor, J.L. Microbiological, chemical, and mineralogical characterization of the Kidd Creek mine tailings impoundment, Timmins area, Ontario. *Geomicrobiol. J.* **1995**, *13*, 13–31.
50. Malmström, M.; Banwart, S. Biotite dissolution at 25 °C: The pH dependence of dissolution rate and stoichiometry. *Geochim. Cosmochim. Acta* **1997**, *61*, 2779–2799.
51. Banfield, J.F.; Eggleton, R.A. Transmission electron microscope study of biotite weathering. *Clays Clay Miner.* **1988**, *36*, 47–60.
52. Kalinowski, B.E.; Schweda, P. Kinetics of muscovite, phlogopite, and biotite dissolution and alteration at pH 1–4, room temperature. *Geochim. Cosmochim. Acta* **1996**, *60*, 367–385.
53. Malmström, M.; Banwart, S.; Lewenhagen, J.; Duro, L.; Bruno, J. The dissolution of biotite and chlorite at 25 °C in the near-neutral pH region. *J. Contam. Hydrol.* **1996**, *21*, 201–213.
54. Barker, W.W.; Welch, S.A.; Chu, S.; Banfield, J.F. Experimental observations of the effects of bacteria on aluminosilicate weathering. *Am. Mineral.* **1998**, *83*, 1551–1563.
55. Murakami, T.; Utsunomiya, S.; Yokoyama, T.; Kasama, T. Biotite dissolution processes and mechanisms in the laboratory and in nature: Early stage weathering environment and vermiculitization. *Am. Mineral.* **2003**, *88*, 377–386.

56. Taylor, A.S.; Blum, J.D.; Lasaga, A.C.; MacInnis, I.N. Kinetics of dissolution and Sr release during biotite and phlogopite weathering. *Geochim. Cosmochim. Acta* **2000**, *64*, 1191–1208.
57. Mycroft, J.R.; Nesbitt, H.W.; Pratt, A.R. X-ray photoelectron and Auger electron spectroscopy of air-oxidized pyrrhotite: Distribution of oxidized species with depth. *Geochim. Cosmochim. Acta* **1995**, *59*, 721–733.
58. Mikhlin, Y.L.; Kuklinskiy, A.V.; Pavlenko, N.I.; Varnek, V.A.; Asanov, I.P.; Okotrub, A.V.; Selyutin, G.E.; Solovyev, L.A. Spectroscopic and XRD studies of the air degradation of acid-reacted pyrrhotites. *Geochim. Cosmochim. Acta* **2002**, *66*, 4057–4067.
59. Wunderly, M.D.; Blowes, D.W.; Frind, E.O.; Ptacek, C.J. Sulfide mineral oxidation and subsequent reactive transport of oxidation products in mine tailings impoundments: A numerical model. *Water Resour. Res.* **1996**, *32*, 3173–3187.
60. Brookfield, A.E.; Blowes, D.W.; Mayer, K.U. Integration of field measurements and reactive transport modelling to evaluate contaminant transport at a sulfide mine tailings impoundment. *J. Contam. Hydrol.* **2006**, *88*, 1–22.

© 2014 by the authors; licensee MDPI, Basel, Switzerland. This article is an open access article distributed under the terms and conditions of the Creative Commons Attribution license (<http://creativecommons.org/licenses/by/3.0/>).